

AD-A106 071

IIT RESEARCH INST CHICAGO IL
TANK CAR HEAD SHIELD FATIGUE PERFORMANCE STUDY.(U)
SEP 81 M R JOHNSON

F/G 13/6

DAAK11-78-C-0043

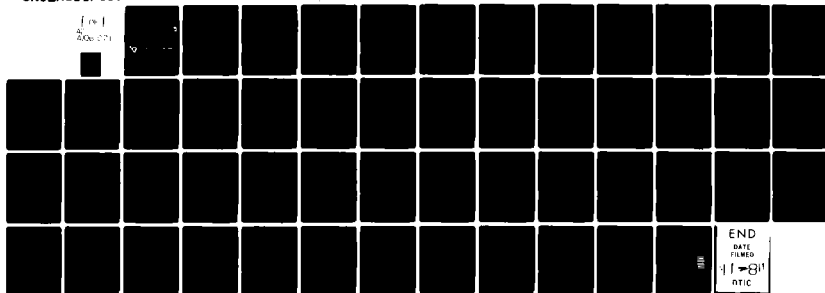
UNCLASSIFIED

IITRI-T06004

ARBRL-CR-00469

NL

1 of 1
5000000



LEVEL

12

AD

AD A106071

CONTRACT REPORT ARBRL-CR-00469

**TANK CAR HEAD SHIELD FATIGUE
PERFORMANCE STUDY**

Prepared by

IIT Research Institute
10 West 35th Street
Chicago, IL 60616

DTIC
ELECTE
OCT 22 1981
D
H

September 1981

DTIC FILE COPY



US ARMY ARMAMENT RESEARCH AND DEVELOPMENT COMMAND
BALLISTIC RESEARCH LABORATORY
ABERDEEN PROVING GROUND, MARYLAND

Approved for public release; distribution unlimited.

81 10 22

Destroy this report when it is no longer needed.
Do not return it to the originator.

Secondary distribution of this report by originating
or sponsoring activity is prohibited.

Additional copies of this report may be obtained
from the National Technical Information Service,
U.S. Department of Commerce, Springfield, Virginia
22151.

The findings in this report are not to be construed as
an official Department of the Army position, unless
so designated by other authorized documents.

*The use of trade names or manufacturers' names in this report
does not constitute endorsement of any commercial product.*

UNCLASSIFIED

SECURITY CLASSIFICATION OF THIS PAGE (When Data Entered)

REPORT DOCUMENTATION PAGE		READ INSTRUCTIONS BEFORE COMPLETING FORM
1. REPORT NUMBER CONTRACT REPORT ARBRL-CR-00469	2. GOVT ACCESSION NO. A2-A706	3. RECIPIENT'S CATALOG NUMBER 071
4. TITLE (and Subtitle) TANK CAR HEAD SHIELD FATIGUE PERFORMANCE STUDY	5. TYPE OF REPORT & PERIOD COVERED 9 Final Report	
7. AUTHOR(s) Milton R. Johnson	6. PERFORMING ORG. REPORT NUMBER DAAK11-78-C-0043	
9. PERFORMING ORGANIZATION NAME AND ADDRESS IIT Research Institute 10 West 35th Street Chicago, IL 60616	10. PROGRAM ELEMENT, PROJECT, TASK AREA & WORK UNIT NUMBERS	
11. CONTROLLING OFFICE NAME AND ADDRESS US Army Armament Research & Development Command US Army Ballistic Research Laboratory (DRDAR-BL) Aberdeen Proving Ground, MD 21005	12. REPORT DATE 11 SEPTEMBER 1981	
14. MONITORING AGENCY NAME & ADDRESS (if different from Controlling Office)	13. NUMBER OF PAGES 42	
	15. SECURITY CLASS. (of this report) UNCLASSIFIED	
16. DISTRIBUTION STATEMENT (of this Report) Approved for public release; distribution unlimited.		
17. DISTRIBUTION STATEMENT (of the abstract entered in Block 20, if different from Report)		
18. SUPPLEMENTARY NOTES		
19. KEY WORDS (Continue on reverse side if necessary and identify by block number) railroad tank cars head shields fatigue hazardous materials tank car		
20. ABSTRACT (Continue on reverse side if necessary and identify by block number) The dynamic response of a typical railroad tank car head shield and its attachments was examined during car-coupling impact tests to determine its expected fatigue performance. The work was based on data obtained on car-coupling impact tests. The test car and one of its head shields were instrumented with transducers to provide a continuous output of strains, forces, and accelerations. The largest strains were measured on the anvil car tests, which was a test where the instrumented car was struck by a moving car. A dynamic finite element analysis was conducted to provide a means for extrapo-		

DD FORM 1 JAN 73 1473 EDITION OF 1 NOV 65 IS OBSOLETE

UNCLASSIFIED

SECURITY CLASSIFICATION OF THIS PAGE (When Data Entered)

cont'd
UNCLASSIFIED

SECURITY CLASSIFICATION OF THIS PAGE(When Data Entered)

Block 20. (Cont'd)

Plating experimental strain data to other locations in the head shield structure. The analysis showed that the maximum strains were about twice the maximum measured strains. The fatigue analysis of the head shield and support structure was restricted to an examination of the effects of car-coupling impacts. The total expected fatigue damage was expressed as the sum of the percentages of fatigue damage in each strain range. The calculation predicted that the annual damage was a very small percentage of the expected fatigue life, being less than 0.2 percent. From a practical standpoint it was concluded that the head shield would have an infinite fatigue life.

UNCLASSIFIED

SECURITY CLASSIFICATION OF THIS PAGE(When Data Entered)

Notice

This document is disseminated under the sponsorship of the Department of Transportation in the interest of information exchange. The United States Government assumes no liability for the contents or use thereof.

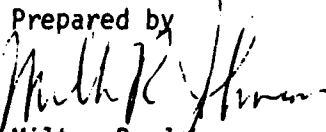
Accession For	
NTIS GRA&I	<input checked="checked" type="checkbox"/>
DTIC TAB	<input type="checkbox"/>
Unannounced	<input type="checkbox"/>
Justification	
By _____	
Distribution/	
Availability Codes	
DISC _____	
A	

PREFACE

This report describes the results of a fatigue evaluation of a head shield for a hazardous material tank car. The work was conducted by IIT Research Institute (IITRI) under the authorization of ARRADCOM Contract DAAK11-78-C-0043, for the U.S. Army Ballistic Research Laboratory (BRL), Aberdeen Proving Ground, Maryland. Dr. Milton R. Johnson has been the IITRI Project Manager.

~~This report is submitted as the second volume of the final report. The first volume was submitted earlier. It described the final results of the Accelerated Life Test which evaluated the long term serviceability of thermal shields and head shields installed on hazardous material tank cars. Dr. Charles Anderson was the cognizant BRL technical monitor. His helpful suggestions and guidance during the course of the work are gratefully acknowledged.~~

Prepared by


Milton R. Johnson
Senior Engineering Advisor
Transportation Research

APPROVED:

Milton Pikarsky
Director, Transportation Research Division

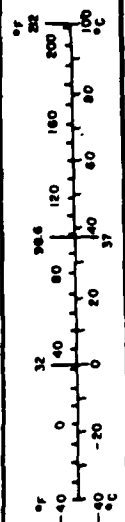
METRIC CONVERSION FACTORS

Approximate Conversions to Metric Measures

Symbol	When You Know	Multiply by	To Find	Symbol
LENGTH				
in	inches	2.5	centimeters	cm
ft	feet	30	centimeters	cm
yd	yards	0.9	meters	m
mi	miles	1.6	kilometers	km
AREA				
sq in	square inches	6.5	square centimeters	cm ²
sq ft	square feet	0.09	square meters	m ²
sq yd	square yards	0.8	square meters	m ²
sq mi	square miles	2.6	square kilometers	km ²
	acres	0.4	hectares	ha
MASS (weight)				
oz	ounces	28	grams	g
lb	pounds	0.45	kilograms	kg
	short tons (2000 lb)	0.9	tonnes	t
VOLUME				
teaspoon	teaspoons	5	milliliters	ml
tablespoon	tablespoons	15	milliliters	ml
fluid ounces	fluid ounces	30	milliliters	ml
cup	cups	0.24	liters	l
pint	pints	0.47	liters	l
quart	quarts	0.95	liters	l
gallon	gallons	3.8	liters	l
cu ft	cubic feet	0.03	cubic meters	m ³
cu yd	cubic yards	0.76	cubic meters	m ³
TEMPERATURE (exact)				
°F	Fahrenheit temperature	5/9 (after subtracting 32)	Celsius temperature	°C

Approximate Conversions from Metric Measures

Symbol	When You Know	Multiply by	To Find	Symbol
LENGTH				
mm	millimeters	0.04	inches	in
cm	centimeters	0.4	inches	in
m	meters	3.3	feet	ft
km	kilometers	1.1	miles	mi
		0.6	miles	mi
AREA				
cm ²	square centimeters	0.16	square inches	sq in
m ²	square meters	1.2	square yards	sq yd
km ²	square kilometers	0.4	square miles	sq mi
ha	hectares (10,000 m ²)	2.5	acres	ac
MASS (weight)				
g	grams	0.035	ounces	oz
kg	kilograms	2.2	pounds	lb
t	tonnes (1000 kg)	1.1	short tons	st
VOLUME				
ml	milliliters	0.03	fluid ounces	fl oz
l	liters	2.1	pints	pt
l	liters	1.06	quarts	qt
m ³	cubic meters	0.26	gallons	gal
m ³	cubic meters	36	cubic feet	cu ft
m ³	cubic meters	1.3	cubic yards	cu yd
TEMPERATURE (exact)				
°C	Celsius temperature	9/5 (then add 32)	Fahrenheit temperature	°F



* 1 in. = 2.54 in. (exact). For other exact temperatures and mass-related factors, see NIST Spec. Publ. 280, Units of Weights and Measures, Part 2, 28, SI Catalog No. C-110, 286.

TABLE OF CONTENTS

	Page
EXECUTIVE SUMMARY	1
1. INTRODUCTION	3
1.1 Objective	3
1.2 Background	3
2. SUMMARY OF TEST PROCEDURES AND RESULTS	4
2.1 Procedures	4
2.2 Instrumentation	4
2.3 Results	10
2.4 Implications of Test Data	10
3. DYNAMIC ANALYSIS	14
3.1 Formulation	14
3.2 Comparison of Theoretical and Experimental Results	14
3.3 Predicted Strains at Other Head Shield Locations	14
4. FATIGUE ANALYSIS	19
4.1 Estimated Number of Car-Coupling Impacts	19
4.2 Analytic Procedures	19
5. CONCLUSIONS	38
6. REFERENCES	39

LIST OF ILLUSTRATIONS

Figure	Page
1. Front View of Head Shield Plate	5
2. Head Shield Attachment Details	6
3. Strain Gauge Positions on Head Shield	8
4. Rosette Strain Gauge Placement on Bracket	9
5. Illustration of 20 Percent Decay Per Half Cycle in Strain Amplitude	13
6. Finite Element Mesh Representation of Head Shield	15
7. Section of Head Shield Plate at Bracket Showing Location of Largest Strain	34

LIST OF TABLES

	Page
1. Instrumentation Used on Tank Car Head Shield Tests	7
2. Maximum Strains Recorded on Test No. 53, 4.1 m/s (9.1 mph) Anvil Car Test	11
3. Maximum Principal Strains Recorded at Gauge Position 2	12
4. Comparison of Results from Test Run No. 6 and Predictions for Peak Strain Data	16
5. Comparison of Results from Test Run No. 29 and Predictions for Peak Strain Data	17
6. Comparison of Maximum Principal Strains Predicted by Dynamic Analysis	18
7. Average Number of Yard Coupling Impacts Per Year (Ref 2)	20
8. Estimated Average Maximum Principal Strains for 3.8 m/s (8.5 mph) Coupling Impact Speed at Gauge Position 2	21
9. Strain Cycles Associated with Car Coupling Impacts for Different Impact Speeds	23
10a. Expected Yearly Number of Strain Cycles - (Hammer Car Impact Condition, Head Shield Opposite Struck End, Front Face)	25
10b. Expected Yearly Number of Strain Cycles - (Hammer Car Impact Condition, Head Shield Opposite Struck End, Rear Face)	26
10c. Expected Yearly Number of Strain Cycles - (Hammer Car Impact Condition, Head Shield at Struck End, Front Face)	27
10d. Expected Yearly Number of Strain Cycles - (Hammer Car Impact Condition, Head Shield at Struck End, Rear Face)	28
10e. Expected Yearly Number of Strain Cycles - (Anvil Car Impact Condition, Head Shield Opposite Struck End, Front Face)	29
10f. Expected Yearly Number of Strain Cycles - (Anvil Car Impact Condition, Head Shield Opposite Struck End, Rear Face)	30
10g. Expected Yearly Number of Strain Cycles - (Anvil Car Impact Condition, Head Shield at Struck End, Front Face)	31
10h. Expected Yearly Number of Strain Cycles - (Anvil Car Impact Condition, Head Shield at Struck End, Rear Face)	32
11. Summary of Expected Yearly Number of Strain Cycles - (Strain Ranges Adjusted for Estimate at Most Highly Stressed Locations)	33
12. Estimated Yearly Fatigue Damage	37

EXECUTIVE SUMMARY

The dynamic response of a typical railroad tank car head shield and its attachments was examined during car-coupling impact tests. This condition leads to the largest stresses which are found in the railroad operating environment. The purpose of the examination was to determine the expected fatigue performance of the head shield. The work was based on data obtained on car-coupling impact tests which were conducted by the U.S. Army, Ballistic Research Laboratory (BRL) at Aberdeen Proving Ground, Md. The data obtained from these tests showed that currently applicable head shield specifications were met, but that some questions remained regarding other factors that should be considered in the fatigue evaluation.

The BRL tests were run under various coupling conditions on a Class 112A tank car equipped with head shields designed by RAILGARD, INC. The test car and one of its two head shields were instrumented with transducers to provide a continuous output of strains, forces, and accelerations. The largest strains were measured on the anvil car tests, which was a test where the instrumented car was struck by a moving car. This was in agreement with similar measurements that were made on other tests. The effect is due to the complex dynamic response phenomena which occur as the struck car is being accelerated after being hit by the moving car.

The largest strains which were recorded during the tests were measured at a gauge location on the head shield plate near the bracket where it was attached to the stub sill. Since it was likely that the gauges were not located exactly at the most highly stressed location, the fatigue evaluation required consideration of the anticipated strains at other positions.

A dynamic finite element analysis was conducted to provide a means for extrapolating experimental strain data to other locations in the head shield structure. The analysis showed that the highest strains in the shield would be reached at a point about 51 mm (2 in.) below and 51 mm (2 in.) toward the center of the shield from the gauge position where the maximum strains were recorded. The maximum predicted strains at this location were about twice the value of the strains predicted for the gauge location. This factor was used to scale up the experimental test data to get an estimate of the maximum strains.

The fatigue analysis of the head shield and support structure was restricted to an examination of the effects of car-coupling impacts. A previous study of head shield fatigue concluded that this is the most important aspect of the railroad service environment for the accumulation of fatigue damage. The analysis was conducted by estimating the number of strain cycles on a yearly basis and then estimating the fatigue damage caused by these cycles. The fatigue damage was expressed as a percentage of the total estimated fatigue life of the structure.

A linear cumulative damage law was assumed for the fatigue damage calculations. The calculation included a determination of the expected number of cycles at various levels of cyclic strain and estimating the percentage of fatigue damage for each of these levels. The total expected fatigue damage was expressed as the sum of the percentages of fatigue damage in each strain

range. The calculation predicted that the annual damage was a very small percentage of the expected fatigue life, being less than 0.2 percent. From a practical standpoint it was concluded that the head shield would have an infinite fatigue life.

The results show that one cannot rely on strain gauge data alone to assess the adequacy of the head shield structure to resist fatigue damage effects. Finite element analysis should be used to interpolate and extrapolate the test data to other locations on the shield. This allows a more complete fatigue evaluation to be made.

1. INTRODUCTION

1.1 Objective

The objective of this program was to make a detailed examination of the fatigue performance of a typical railroad tank car head shield and its attachments when subjected to the car-coupling impact environment. This is the operating environment which leads to the largest stresses within the shield and its supporting structure. The work was based on test data obtained on car-coupling impact tests which were conducted by the U.S. Army, Ballistic Research Laboratory (BRL) at Aberdeen Proving Ground, Md. The data obtained from these tests showed that currently applicable head shield specifications were met, but that some questions remained regarding other factors that should be considered in the fatigue evaluation.

The primary factor which had to be examined in the fatigue performance evaluation was the number and range of strain cycles which are associated with car-coupling impact. The number and range of strain cycles is known to be a function of the car-coupling impact speed, the higher speeds leading to the more severe cases. Data were available giving the average number of coupling impacts that a tank car encounters in a typical year's operation. The fatigue properties of the shield were then to be evaluated at the critical regions where strain gauges were placed. Utilizing the summary of stress cycles and a fatigue analysis, the service life of the head shield was predicted. The principal result from this analysis was a determination whether or not the anticipated fatigue life of the structure was finite or infinite.

A second factor which had to be considered in the evaluation was to determine the location of the maximum strains in the head shield and in this way identify the most critical region. On impact tests it is impossible to include strain gauges at every location on the structure. Therefore, it is important to determine whether or not regions of stress concentration will produce higher strains than those indicated by the strain gauges. This factor was examined by conducting a dynamic finite element analysis of a typical severe car-coupling impact and using the results to provide a basis for extrapolating the measured strains to other regions of the structure.

1.2 Background

The head shield tests conducted at BRL were run under various conditions of car-coupling impacts. Strain gauge and accelerometer data were obtained. The immediate purpose of these tests was to determine whether or not the head shield design was in compliance with the specifications set forth by the Association of American Railroads (AAR) for evaluating new head shield designs (Ref 1). The test procedures and results are described in a separate report (Ref 2).

2. SUMMARY OF TEST PROCEDURES AND RESULTS

2.1 Procedures

A head shield designed by RAILGARD, INC. was installed on a 45.4 kl (12,000 gallon) classification 112A tank car. The test car and one of its two head shields were instrumented with transducers to provide a continuous output of strains, forces, and accelerations. The car was tested both as an anvil car and as a hammer car*. The orientation of the car was also changed so that some tests were made with the instrumented shield at the struck end of the car and other tests with it at the opposite end. The impact tests under each set of conditions were begun at approximately 1.8 m/s (4 mph) and the speed was increased in 0.45 m/s (1 mph) increments for subsequent tests until a coupler force of 5.56 MN (1,250,000 lbs) was reached as required in the AAR specifications (Ref 1).

The test car had the following characteristics:

Owner's No.	PSPC 21725
Classifications	112A400W
Service	Anhydrous Ammonia
Built	January 1958
Tank Capacity	55.48 kl (14,656 gallons)
Capacity	49.4 Mg (110,000 lbs)
Light Weight	30.1 Mg (66,400 lbs)
Water Capacity	55.36 Mg (122,059 lbs)

The car was equipped with Barber S-2 trucks having 140 x 254 mm (5-1/2 x 10 in.) plain bearing journals.

The head shields were installed at both ends of the car. Details of the design are shown in Figures 1 and 2. The bottom of the head shield is bolted to two brackets which are welded to the center sill. The sides of the head shield are supported by struts which are connected to the bolster.

2.2 Instrumentation

Accelerometers, strain gauges, and dynamometer couplers were applied to the test car. Table 1 summarizes the instrumentation plan.

Strain gauges were applied to the head shield and its supporting attachments as a means of evaluating the dynamic stresses occurring in the shield under car-coupling impact conditions and to provide a basis for estimation of the dynamic loads transmitted through the attachments. (Only the shield at one end of the car was instrumented with strain gauges.) Figure 3 shows the positions where strain gauges were applied. These positions include regions where a preliminary analysis indicated large stresses would occur. Figure 4 shows the rosette strain gauge position on the bracket. A single element strain gauge was applied to each of the side support tubes (Figure 2); these were placed parallel to the axis of the tube. Micro-measurements types CEA-06-125UW-350 (single element) strain gauges were used.

*On an anvil car test, the test car is struck by a moving car; on a hammer car test the test car is moving and strikes a standing car. See test report (Ref 2) for details.

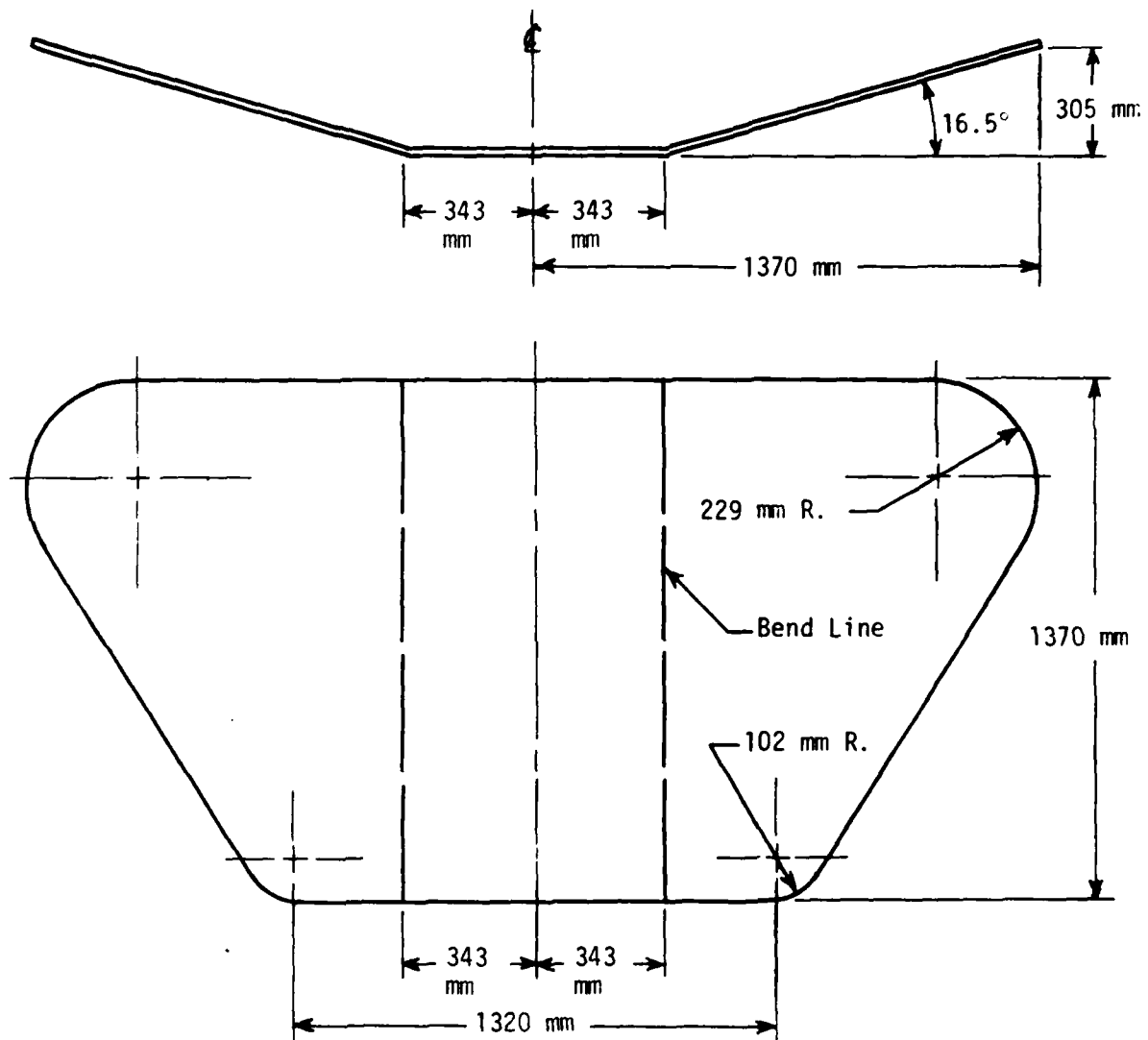


FIGURE 1. FRONT VIEW OF HEAD SHIELD PLATE

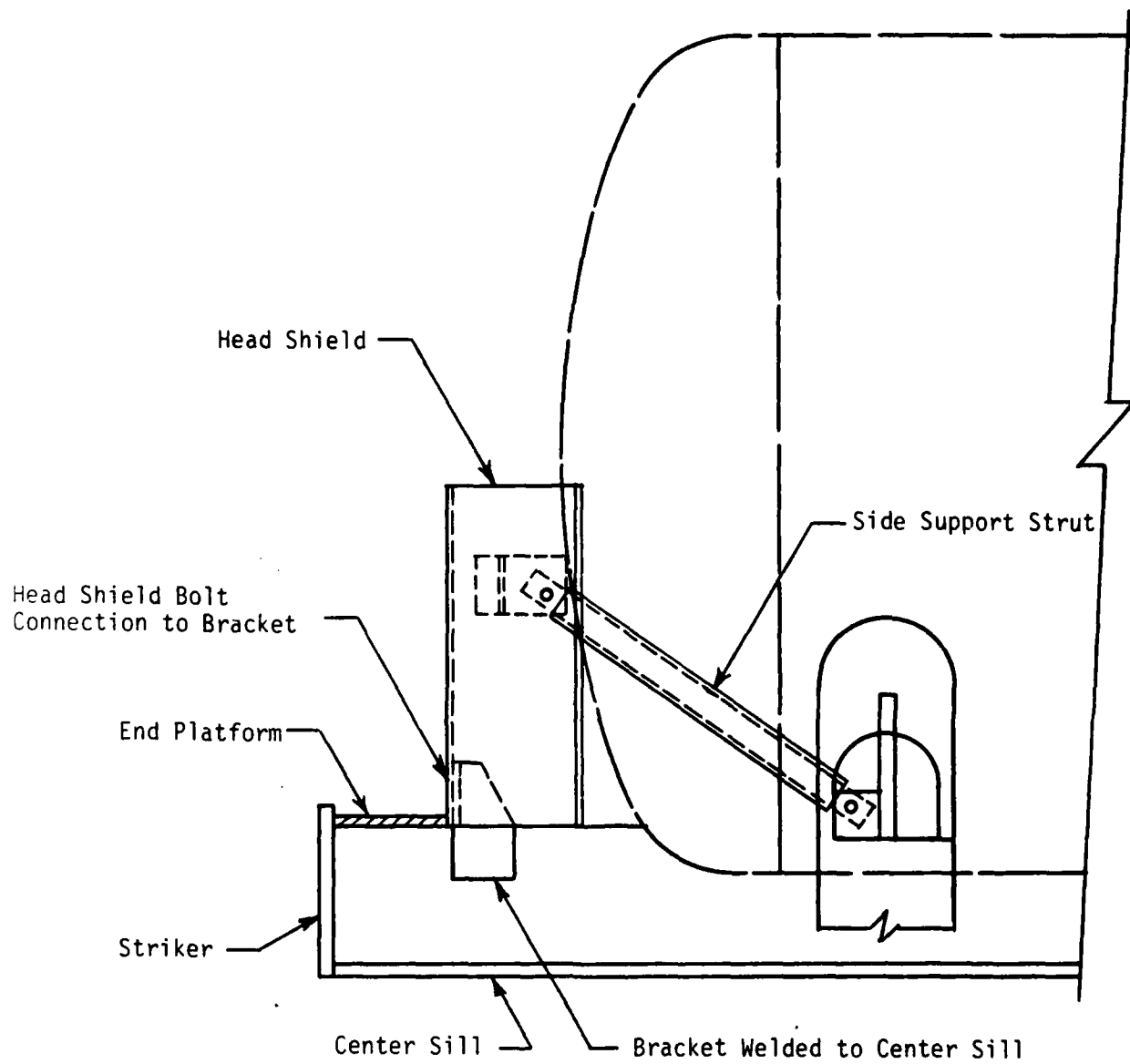


FIGURE 2. HEAD SHIELD ATTACHMENT DETAILS

TABLE 1. INSTRUMENTATION USED ON TANK CAR HEAD SHIELD TESTS

Gauge Channel No.	Type	Orientation (V: Vertical H: Horizontal S: Slant)	Gauge Position (See Figs. 2, 3 and 4)	Location
1	Strain	V		Left
2	Gauge	S	2	Side
3	Rosette	H		Front
4	Strain	V		Left
5	Gauge	S	2	Side
6	Rosette	H		Rear
7	Strain	V		Right
8	Gauge	S	2	Side
9	Rosette	H		Front
10	Strain	V		Right
11	Gauge	S	2	Side
12	Rosette	H		Rear
13	Strain	V		Right
14	Gauge	S	1	Side
15	Rosette	H		Front
16	Strain	V		Right
17	Gauge	S	1	Side
18	Rosette	H		Rear
19	Strain	V		Left
20	Gauge	S	5	Stub Sill
21	Rosette	H		Bracket
22	Strain	V		Right
23	Gauge	S	5	Stub Sill
24	Rosette	H		Bracket
25	Single Element	Along	6	Left Strut Support
26	Strain Gauges	Axis		Right Strut Support
27	Single Element	H	3	Front Center
28	Strain	H	4	Left Side*
29	Gauges	H	4	Right Side*
30	Dynamometer	H	-	Instrumented End
31	Couplers (force)	H	-	Noninstrumented End
32		V	-	Instrumented End
33	Accelerometers	H	-	Instrumented End
34		V	-	Noninstrumented End

*Single gauges on front and back side wired into a two-active-arm strain gauge bridge sensitive to bending in the plate.

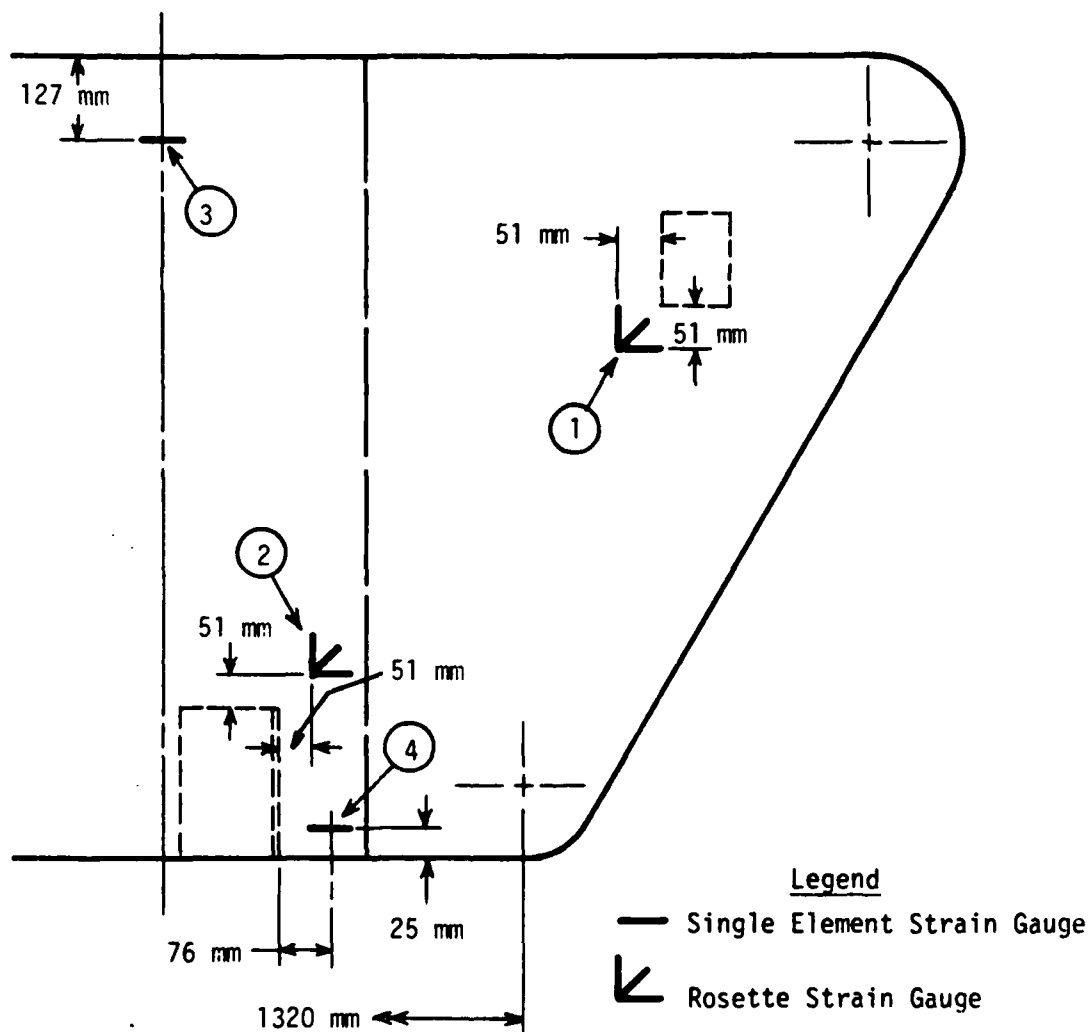


FIGURE 3. STRAIN GAUGE POSITIONS ON HEAD SHIELD

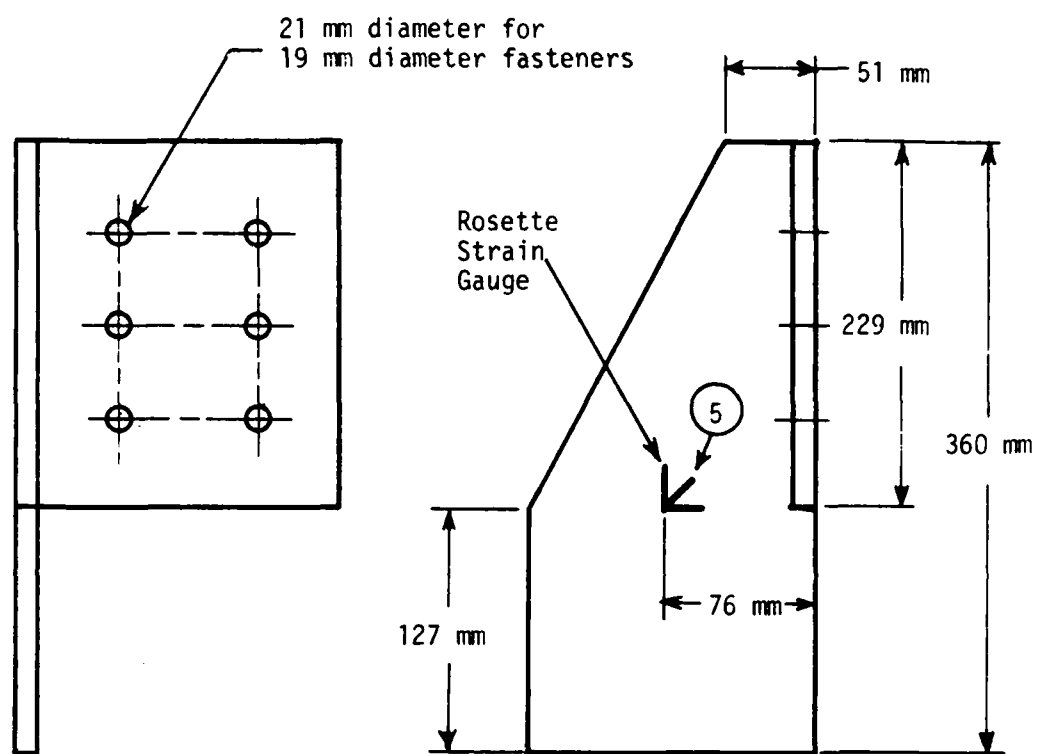


FIGURE 4. ROSETTE STRAIN GAUGE PLACEMENT ON BRACKET

2.3 Results

The largest strains were measured at gauge Position 2. It had been anticipated that this was the region in which the highest strains would be recorded. Table 2 compares the strains measured at Position 2 and those measured at other gauge locations on the shield and the supporting bracket. It demonstrates that the strains at Position 2 were the largest. The data in this table are shown for test run Number 53, a 4.1 m/s (9.1 mph) anvil car test where the impact occurred at the non-instrumented end of the car.

The strains measured at Position 2 were different for the various types of car-coupling tests. This is illustrated in Table 3 where the strains measured at Position 2 are shown for the tests which were conducted in the vicinity of 3.6 m/s (8.0 mph), the nominal maximum impact speed used on the test program. The data shown in the table for the hammer car tests pertain to the first recorded peak since on these tests the maximum value was recorded on the first half cycle. The absolute values of each succeeding peak were reduced in magnitude. On the three types of anvil car tests this was not the case; the second peak was often larger than the first peak. This is illustrated by including the maximum principal strains for both the first peak and the second peak of the cyclic data for the tests. The measurement of larger strains on the anvil car tests is in agreement with similar measurements that were made on another series of tests (see Ref 3). The effect is due to the complex dynamic response phenomena which occur as the struck car is accelerated after being hit by the moving car.

The decay rates were analyzed for each of the cases listed in Table 3. It was found that there was no substantial difference in the rate of decay from one cycle to the next for the two different types of tests, hammer car or anvil car test, although there was some variation from run to run and from one channel to another. The average decay rate, however, was essentially the same for each case if one looked at the decay following the first peak for the hammer car tests and following the second peak for the anvil car tests. In both cases each succeeding half cycle was about 80 percent of the amplitude of the preceding local peak value. This is illustrated in Figure 5. The test data indicated a range in the attenuation factor from 0.7 to 0.9, but there was no correlation between its value and the conditions of the test.

2.4 Implications of Test Data

A previous report, Ref 2, reviewed the test data with respect to the AAR specifications for head shield design. The analysis was based on the strain gauge readings at Position 2. The results of this analysis showed that the head shield passed the requirements.

It was likely, however, that the strain gauges at Position 2 were not at the most highly stressed location on the head shield. A thorough examination of the fatigue properties of the shield had to assess the possibility that there would be a more rapid accumulation of fatigue damage at other positions.

TABLE 2. MAXIMUM STRAINS RECORDED ON TEST NO. 53,
4.1 m/s (9.1 mph) ANVIL CAR TEST

Gauge Location (See Figs. 3 and 4)	Maximum Strain μ mm/mm (μ in./in.)
Position 2 (average right and left sides)	
Front Face	-1580*
Rear Face	1800*
Position 1	
Front Face	980*
Rear Face	-1150*
Position 3	+ 620 - 620
Position 4 (average right and left sides, front and rear faces)	+ 880 - 880
Position 5 (on support bracket)	
Left Side	- 620*
Right Side	- 520*

*Principal Strains

TABLE 3. MAXIMUM PRINCIPAL STRAINS RECORDED AT GAUGE POSITION 2

Type of Test	Impacted End of Car	Test No.	Speed m/s (mph)	Cycle Peak	Maximum (Absolute) Strain μ mm/mm (μ in./in.)	
					Front Face	Rear Face
Hammer Car	Noninstr. End	6	3.7 (8.3)	1	1063	-1087
		7	3.9 (8.8)	1	1194	-1164
		8	3.9 (8.7)	1	1169	-1077
	Instr. End	14	3.8 (8.6)	1	- 809	882
		15	3.9 (8.8)	1	- 855	936
Anvil-Free-to-Roll	Noninstr. End	21	3.6 (8.1)	1	1373	-1336
				2	-1355	1649
		22	3.6 (8.1)	1	1370	-1420
				2	-1224	1450
	Instr. End	29	3.6 (8.0)	1	- 816	862
				2	789	- 840
		30	3.7 (8.2)	1	- 825	926
				2	901	- 914
Anvil - Not Separated	Instr. End	37	3.5 (7.9)	1	- 887	923
				2	1226	-1163
	Noninstr. End	50	3.6 (8.0)	1	1298	-1228
				2	-1361	1507
Anvil - Separated by 2.4 m (8 ft)	Instr. End	39	3.6 (8.1)	1	- 885	973
				2	1192	-1058
		42	3.4 (7.6)	1	- 735	860
				2	1359	-1292
	Noninstr. End	51	3.5 (7.8)	1	1299	-1303
				2	-1378	1580
		53	4.1 (9.1)	1	1491	-1401
				2	-1575	1796

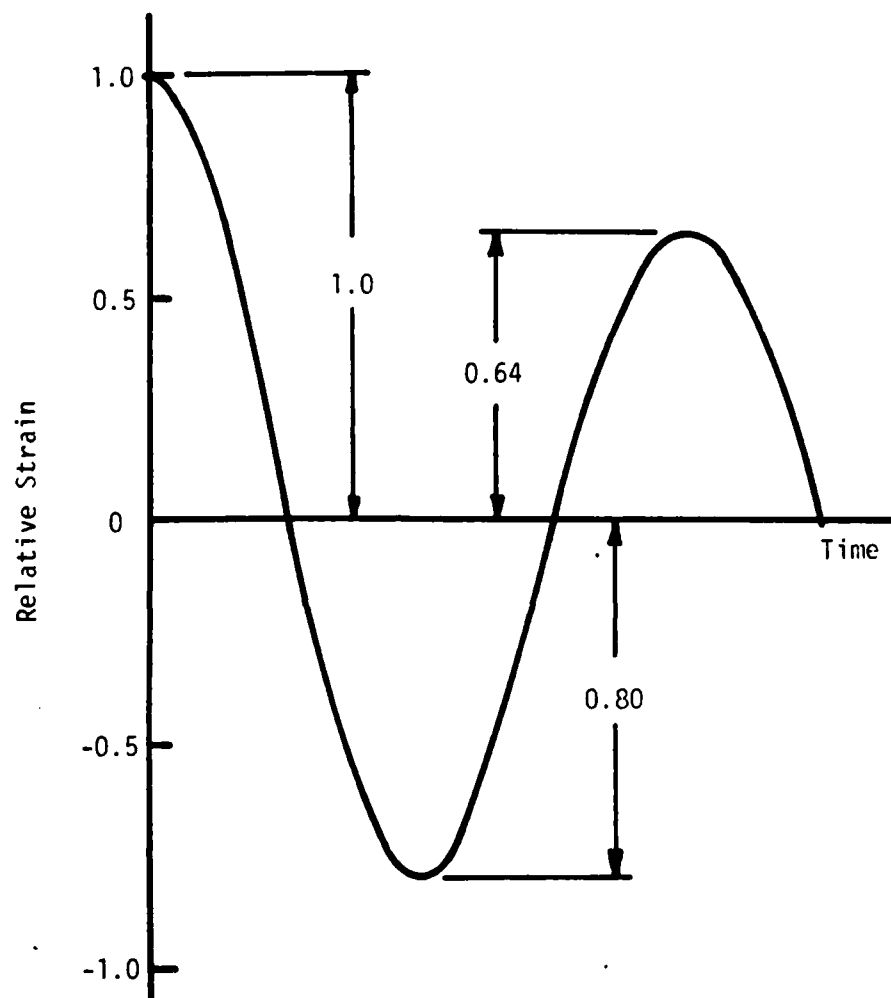


FIGURE 5. ILLUSTRATION OF 20 PERCENT DECAY
PER HALF CYCLE IN STRAIN AMPLITUDE

3. DYNAMIC ANALYSIS

3.1 Formulation

A dynamic analysis was conducted to provide a means for extrapolating experimental strain data recorded during the car-coupling tests to other locations in the head shield structure.

A finite element model was constructed of the head shield. It utilized beam and plate elements. A preliminary analysis was conducted to estimate the regions of the shield where there were large stress gradients. The mesh was then modified to utilize smaller elements where there were regions of stress concentration and large stress gradients. The final mesh is shown in Figure 6. Note that the model was constructed with the assumption that the shield was symmetric about the center line of the car.

The assumption was made that the acceleration of the car could be inferred from the coupler force measured at the struck end of the car. The dynamic excitation of the shield was then caused by this motion. It should be recognized that there were several limitations in this procedure. First of all, it was not certain if the support points at the base of the shield and the support points at the ends of the struts were in the same phase relationship. Secondly, there was no way to determine the structural damping. An estimate had to be made of this parameter in the analysis. Furthermore, the impact forces acting on the tank car produced a stress wave which moved from one end of the car to the other and was subsequently reflected back towards the point of impact. Thus, the assumption of a rigid body acceleration was only an approximation of the complex phenomena which occurred in the actual case.

3.2 Comparison of Theoretical and Experimental Results

Experimental results from test runs No. 6 and 29 were compared with the dynamic analysis. Test No. 6 was a hammer car test at 3.7 m/s (8.3 mph) with the impact at the non-instrumented end of the car. Test No. 29 was a 3.6 m/s (8.0 mph) anvil car test with the impact at the non-instrumented end of the car. The results are shown in Tables 4 and 5, where maximum strains are given for the first three peaks of the fundamental mode of vibration. Test No. 6 data show an average 15 percent variation between the predicted and measured values. Test No. 29 shows that the predicted values for the first peak are about 30 percent greater than the measured value. The predicted and experimental measurements for the second peak are about the same. The predicted values for the third peak are about 24 percent less than the experimental values.

3.3 Predicted Strains At Other Head Shield Locations

The data from the dynamic analysis can be used to determine the location where the largest strains would be expected on the head shield. An examination of these data show that the largest strains would be reached at a point about 51 mm (2 in.) below and 51 mm (2 in.) toward the center of the shield from Position No. 2 (see Figure 6). The maximum predicted strains at this location are compared with the predicted strains for Position No. 2 in Table 6. The average increase of front face strains is 1.87 and the average increase of back face strains is 1.99. A nominal representation of these two factors, 2.0, was used to scale up the experimental test data from Position No. 2 as an estimate of the largest strain in the head shield.

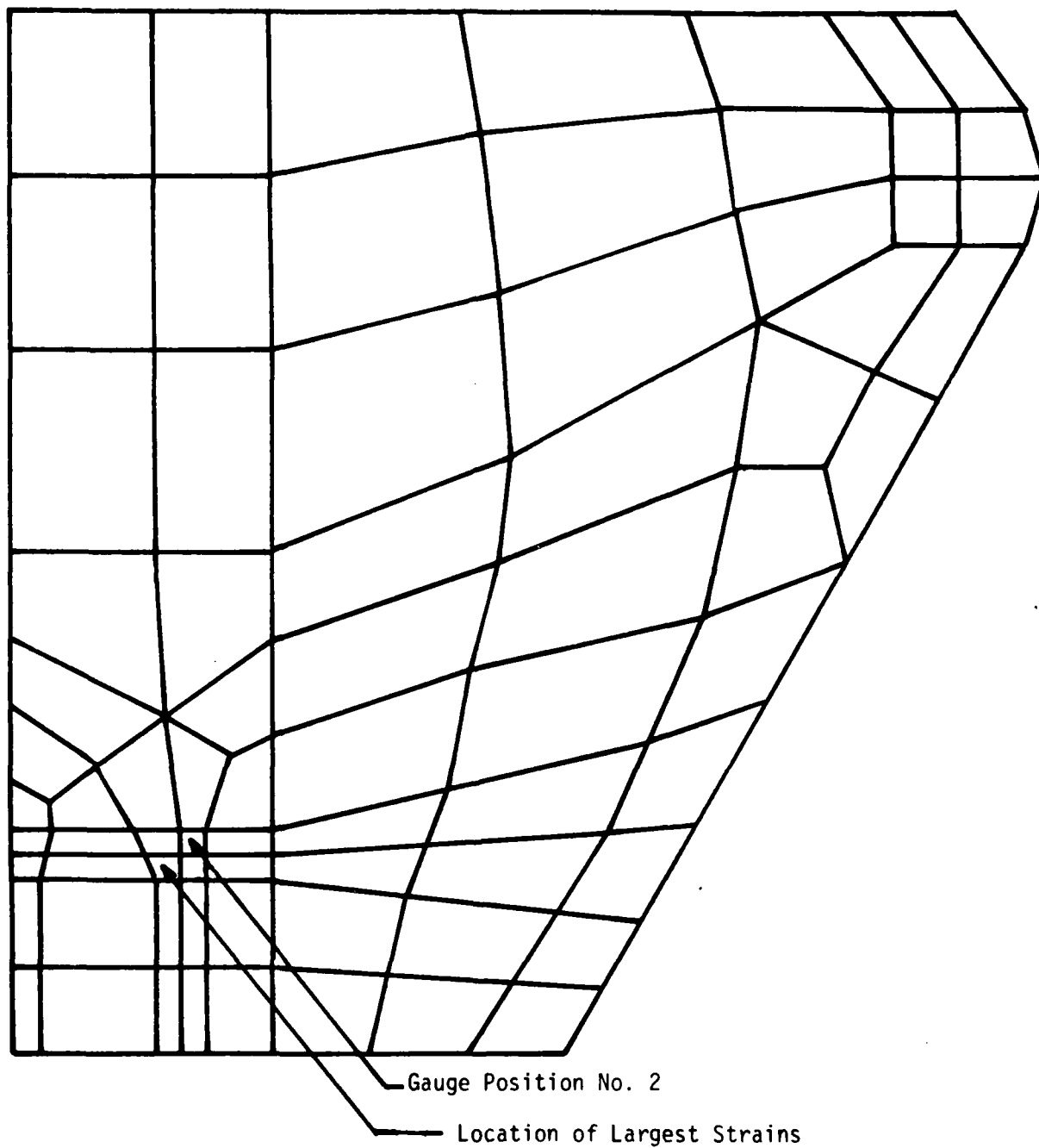


FIGURE 6. FINITE ELEMENT MESH REPRESENTATION OF HEAD SHIELD

TABLE 4. COMPARISON OF RESULTS FROM TEST RUN NO. 6 AND
PREDICTIONS FOR PEAK STRAIN DATA

Gauge Location (See Fig. 3)	Type of Data	Strain, μ mm/mm (μ in./in.)		
		1st Peak	2nd Peak	3rd Peak
Position 2, Vertical Front	Prediction	652	- 560	363
	Exp. Left Side	430	- 300	330
	Exp. Right Side	500	- 290	290
Position 2, Horizontal Front	Prediction	946	- 767	422
	Exp. Left Side	1070	- 710	580
	Exp. Right Side	1020	- 670	600
Position 2, Vertical Rear	Prediction	- 797	683	-439
	Exp. Left Side	- 960	720	-620
	Exp. Right Side	- 950	610	-570
Position 2, Horizontal Rear	Prediction	- 689	547	-280
	Exp. Left Side	- 520	340	-300
	Exp. Right Side	- 740	540	-240
Position 4, Front and Back Gauges Summed	Prediction	1311	-1086	619
	Exp. Left Side	1140	-1080	980
	Exp. Right Side	1030	- 790	880
Position 3, Front Face Gauge	Prediction	- 296	263	-190
	Experimental	- 360	430	-400
Average Ratio of Measured Strains to Predicted Strains (excluding Position 3)		.95	.81	1.22

TABLE 5. COMPARISON OF RESULTS FROM TEST RUN NO. 29 AND
PREDICTIONS FOR PEAK STRAIN DATA

Gauge Location (See Fig. 3)	Type of Data	Strain, μ mm/mm (μ in./in.)		
		1st Peak	2nd Peak	3rd Peak
Position 2, Vertical Front	Prediction	652	- 560	363
	Exp. Left Side	350	- 500	310
	Exp. Right Side	330	- 460	280
Position 2, Horizontal Front	Prediction	946	- 767	422
	Exp. Left Side	860	- 840	920
	Exp. Right Side	680	- 690	610
Position 2, Vertical Rear	Prediction	- 797	683	-439
	Exp. Left Side	- 800	820	-860
	Exp. Right Side	- 700	700	-540
Position 2, Horizontal Rear	Prediction	- 689	547	-280
	Exp. Left Side	- 470	520	-270
	Exp. Right Side	- 550	590	-260
Position 4, Front and Back Gauges Summed	Prediction	1311	-1086	619
	Exp. Left Side	1140	-1130	970
	Exp. Right Side	980	- 760	800
Position 3, Front Face Gauge	Prediction	- 296	263	-190
	Experimental	- 230	660	-540
Average Ratio of Measured Strains to Predicted Strains (excluding Position 3)		.77	.97	1.32

TABLE 6. COMPARISON OF MAXIMUM PRINCIPAL STRAINS
PREDICTED BY DYNAMIC ANALYSIS

Position	Predicted Strain, μ mm/mm (μ in./in.)		
	1st Peak	2nd Peak	3rd Peak
Gauge Position 2 (See Fig. 3):			
Front Face	1030	- 840	470
Rear Face	- 830	710	-460
Position of Largest Predicted Strains:			
Front Face	1890	-1560	900
Rear Face	-1680	1440	-880

4. FATIGUE ANALYSIS

4.1 Estimated Number of Car-Coupling Impacts

Information is available (Ref 3) which provides an estimate of the number of tank car car-coupling impacts per year and the distribution of speeds over which these impacts occur. These data are summarized in Table 7. An average of 62.5 car-coupling impacts per year is predicted. The events listed in this table refer to switching movements. Normally there would be two primary coupling impacts associated with each event. The first one occurs when the car is the moving car striking fixed cars and, second, when the car is the struck car. For example, when a car is humped in a classification yard, it will strike standing cars and the next car humped will strike it leading to a second coupling impact. There will be more coupling impact shocks as additional cars are humped into the string of cars, but the shock effects will be attenuated by the intervening cars.

4.2 Analytic Procedures

The fatigue analysis of the head shield and supporting structure was restricted to an examination of the effects of car-coupling impacts. A previous study of head shield fatigue concluded that this is the most important aspect of the railroad service environment for the accumulation of fatigue damage (Ref 3). A more complete analysis would consider environmental data from both the car-coupling and over-the-road environments.

The fatigue analysis was conducted by determining the expected number of stress (strain) cycles on a yearly basis and then estimating the fatigue damage caused by these cycles. The fatigue damage was expressed as a percentage of the total estimated fatigue life of the structure.

The maximum principal strains measured at Position 2 are shown in Table 3 for each type of car-coupling test. The fatigue analysis was concerned with only two of these test configurations, namely, the hammer car test and the anvil car test (restrained condition). The number of coupling events was determined by assuming that each car-coupling impact listed in Table 7 covers fluctuating strains equivalent to a hammer car test and an anvil car test. It was also assumed that one-half of the impacts occur with the car oriented in one direction and one half of the impacts occur with the car oriented in the opposite direction.

The data in Table 3 were used as a basis for estimating the number and magnitude of the strain cycles. As explained earlier, the half amplitude of each peak following the maximum was only 0.8 of the preceding peak amplitude. The maximum amplitude occurred on the first half cycle of hammer car tests. The maximum amplitude usually took place on the second half cycle of anvil car tests.

The data in Table 3 were also used as a basis for determining the magnitudes of the cyclic strains as a function of the coupling impact speed. Data from previous tests (Ref 3) showed that the maximum amplitude of the cyclic strains scales as the square of the speed on hammer car tests, and as the cube of speed on anvil car tests. Table 8 presents maximum strain data for each test configuration in terms of a 3.8 m/s (8.5 mph) impact speed.

TABLE 7. AVERAGE NUMBER OF YARD COUPLING IMPACTS
PER YEAR (Ref 2)

Speed Range m/s (mph)	Average Number of Coupling Impacts Per Year
0 to 0.9 (0 to 2)	1.0
0.9 to 1.3 (2 to 3)	3.0
1.3 to 1.8 (3 to 4)	9.0
1.8 to 2.2 (4 to 5)	13.0
2.2 to 2.7 (5 to 6)	15.0
2.7 to 3.1 (6 to 7)	10.0
3.1 to 3.6 (7 to 8)	6.0
3.6 to 4.0 (8 to 9)	3.0
4.0 to 4.5 (9 to 10)	1.5
4.5 to 4.9 (10 to 11)	1.0
Total	62.5

TABLE 8. ESTIMATED AVERAGE MAXIMUM PRINCIPAL STRAINS
FOR 3.8 m/s (8.5 mph) COUPLING IMPACT SPEED AT GAUGE POSITION 2

Type of Test	Impacted End of Car	Cyclic Peak	Maximum (Absolute) Strain μ mm/mm (μ in./in.)	
			Front Face	Rear Face
Hammer Car	Noninstr. End	1	1115	-1085
	Instr. End	1	- 794	867
Anvil Free-to-Roll	Noninstr. End	2	-1420	1707
	Instr. End	2	935	- 965
Anvil - Not Separated	Noninstr. End	2	-1632	1808
	Instr. End	2	1527	-1449
Anvil - Separated by 8 Feet	Noninstr. End	2	-1506	1722
	Instr. End	2	1507	-1391

The calculation of the number of strain cycles assumed that a tensile half cycle was followed by a compressive half cycle. Table 9 gives the number of tensile cyclic strain peaks within given strain ranges for each type of test. These tables also show the distributions of these cyclic peaks for various car-coupling speeds. On the anvil car tests an extra half cycle at the peak strain value was added to account for the fact that the maximum strain occurred on the second half cycle.

The total number of strain cycles was estimated on a yearly basis by using the data in Table 9 and the yearly exposure estimate given in Table 7. This information is shown in Tables 10a to 10h for each test condition. Data are also given for both the front face of the shield and the rear face of the shield at Position 2.

The dynamic analysis showed that the principal strains adjacent to gauge Position 2 would be about twice the magnitude measured by the gauges at Position 2. The fatigue analysis was conducted for this most highly stressed location. The measured strains given in Table 10a to 10h were multiplied by two for the calculations. The resulting data are presented in Table 11, where the expected number of strain cycles per year are indicated.

The fatigue problem at the location selected for analysis was obviously a problem in low cycle fatigue because the car-coupling impacts lead to a relatively small number of large amplitude strain cycles. To estimate the fatigue damage effects it was necessary to establish a procedure for determining the expected fatigue damage under these circumstances.

The AAR has published a procedure which is to be followed in the fatigue design of freight car components (Ref 4). The AAR fatigue design procedure is based upon the use of modified Goodman diagrams for particular materials and structural details. These diagrams portray the fatigue limit as a function of the stress ratio. The fatigue limit is assumed to be established at 2×10^6 cycles. A procedure is given for calculating the number of cycles to failure for higher amplitude stress cycles. It is assumed that the number of cycles to failure can be represented by a straight line on a plot of log stress vs log cycles. The slope of such a plot is given for a number of structural details and materials.

The fatigue analysis of the head shield was based on the assumption that it was constructed of ATSM A242 steel having a yield point of 345 MPa (50 ksi). The AAR fatigue design procedures do not contain a modified Goodman diagram which corresponds to the type of structural detail on the head shield at the location where the fatigue damage analysis was to be conducted. There would be a relatively low stress concentration factor at this point because there was no weld penetration into the plate. Maximum plate stresses were developed at the outside edge of the bracket plate which is attached at the center sill of the car. This is illustrated in Figure 7.

The assumption was made that the fatigue properties of the plate material given in the AAR procedures (Figure 7.4.1.1 of Ref 4) could provide a basis for the analysis of fatigue damage. It was also assumed that there were no stress or fatigue concentration factors to consider. Another assumption was made regarding the magnitude of the strain cycles to consider in the fatigue damage calculations. It was assumed that each positive (tensile) strain peak has associated with it a negative (compressive) strain peak of equal magnitude.

TABLE 9. STRAIN CYCLES ASSOCIATED WITH CAR COUPLING
IMPACTS FOR DIFFERENT IMPACT SPEEDS

Test Condition	Impact Speed m/s (mph)	Number of Cyclic Peaks Within Indicated Strain Ranges μ mm/mm (μ in./in.)							
		250 to 500	500 to 750	750 to 1000	1000 to 1500	1500 to 2000	2000 to 2500	2500 to 3000	3000 to 3500
Hammer Car, Head	4.7 (10.5)	2	1		1	1			
Shield Opposite	4.2 (9.5)	1	1	1	1				
Struck End,	3.8 (8.5)	2	1		1				
Front Face	3.4 (7.5)	2	1						
	2.9 (6.5)	2	1						
	2.5 (5.5)	2							
	2.0 (4.5)	1							
Hammer Car, Head	4.7 (10.5)	1	1	1	1				
Shield Opposite	4.2 (9.5)	2	1		1				
Struck End,	3.8 (8.5)	1	1	1					
Rear Face	3.4 (7.5)	2	1						
	2.9 (6.5)	1	1						
	2.5 (5.5)	1							
Hammer Car, Head	4.7 (10.5)	2	1	1					
Shield at Struck	4.2 (9.5)	1	1	1					
End, Front Face	3.8 (8.5)	2	1						
	3.4 (7.5)	2							
	2.9 (6.5)	1							
	2.5 (5.5)	1							
Hammer Car, Head	4.7 (10.5)	1	1	1	1				
Shield at Struck	4.2 (9.5)	2	1		1				
End, Rear Face	3.8 (8.5)	1	1	1					
	3.4 (7.5)	2	1						
	2.9 (6.5)	1	1						
	2.5 (5.5)	1							
Anvil Car, Head	4.7 (10.5)	2	1		1	1	1		
Shield Opposite	4.2 (9.5)	2	1		1	1			
Struck End,	3.8 (8.5)	1	1	1	1				
Front Face	3.4 (7.5)	1	1	1					
	2.9 (6.5)	1	1						
	2.5 (5.5)	1							
Anvil Car, Head	4.7 (10.5)	1	1	1	1		1		1
Shield Opposite	4.2 (9.5)	2	1		1	1		1	
Struck End,	3.8 (8.5)	2	1		1	1			
Rear Face	3.4 (7.5)	1	1	1	1				
	2.9 (6.5)	1	1	1					
	2.5 (5.5)	2							
	2.0 (4.5)	1							

TABLE 9. STRAIN CYCLES ASSOCIATED WITH CAR COUPLING
IMPACTS FOR DIFFERENT IMPACT SPEEDS (Concluded)

Test Condition	Impact Speed m/s (mph)	Number of Cyclic Peaks Within Indicated Strain Ranges μ mm/mm (μ in./in.)							
		250 to 500	500 to 750	750 to 1000	1000 to 1500	1500 to 2000	2000 to 2500	2500 to 3000	3000 to 3500
Anvil Car, Head	4.7 (10.5)	2		1	1	1		1	
Shield at Struck	4.2 (9.5)	1	1	1	1		1		
End, Front Face	3.8 (8.5)	2	1	1		1			
	3.4 (7.5)	2	1		1				
	2.9 (6.5)	2	1						
	2.5 (5.5)	2							
Anvil Car, Head	4.7 (10.5)	1	1	1	1		1		
Shield at Struck	4.2 (9.5)	2	1		1	1			
End, Rear Face	3.8 (8.5)	2	1		1				
	3.4 (7.5)	1	1	1					
	2.9 (6.5)	1	1						
	2.5 (5.5)	1							

TABLE 10a. EXPECTED YEARLY NUMBER OF STRAIN CYCLES
(Hammer Car Impact Condition, Head Shield Opposite Struck End, Front Face)

Speed Range of Coupling Impact m/s (mph)	Number of Events Per Year	Strain Cycles Per Year In Indicated Strain Ranges, μ mm/mm (μ in./in.)							
		250 to 500	500 to 750	750 to 1000	1000 to 1500	1500 to 2000	2000 to 2500	2500 to 3000	3000 to 3500
4.5 to 4.9 (10 to 11)	0.5	1.0	0.5		0.5	0.5			
4.0 to 4.5 (9 to 10)	0.75	0.75	0.75	0.75	0.75				
3.6 to 4.0 (8 to 9)	1.5	3.0	1.5		1.5				
3.1 to 3.6 (7 to 8)	3.0	6.0	3.0						
2.7 to 3.1 (6 to 7)	5.0	10.0	5.0						
2.2 to 2.7 (5 to 6)	7.5	15.0							
1.8 to 2.2 (4 to 5)	6.5	6.5							
Subtotal		31.5	10.7	0.75	2.75	0.5			

TABLE 10b. EXPECTED YEARLY NUMBER OF STRAIN CYCLES
(Hammer Car Impact Condition, Head Shield Opposite Struck End, Rear Face)

Speed Range of Coupling Impact m/s (mph)	Number of Events Per Year	Strain Cycles Per Year In Indicated Strain Ranges, μ mm/mm (μ in./in.)							
		250 to 500	500 to 750	750 to 1000	1000 to 1500	1500 to 2000	2000 to 2500	2500 to 3000	3000 to 3500
4.5 to 4.9 (10 to 11)	0.5	0.5	0.5	0.5	0.5				
4.0 to 4.5 (9 to 10)	0.75	1.5	0.75		0.75				
3.6 to 4.0 (8 to 9)	1.5	1.5	1.5	1.5					
3.1 to 3.6 (7 to 8)	3.0	6.0	3.0						
2.7 to 3.1 (6 to 7)	5.0	5.0	5.0						
2.2 to 2.7 (5 to 6)	7.5	7.5							
Subtotal		22.0	10.75	2.0	1.25				

TABLE 10c. EXPECTED YEARLY NUMBER OF STRAIN CYCLES
(Hammer Car Impact Condition, Head Shield At Struck End, Front Face)

Speed Range of Coupling Impact m/s (mph)	Number of Events Per Year	Strain Cycles Per Year In Indicated Strain Ranges, μ mm/mm (μ in./in.)							
		250 to 500	500 to 750	750 to 1000	1000 to 1500	1500 to 2000	2000 to 2500	2500 to 3000	3000 to 3500
4.5 to 4.9 (10 to 11)	0.5	1.0	0.5	0.5					
4.0 to 4.5 (9 to 10)	0.75	0.75	0.75	0.75					
3.6 to 4.0 (8 to 9)	1.5	3.0	1.5						
3.1 to 3.6 (7 to 8)	3.0	6.0							
2.7 to 3.1 (6 to 7)	5.0	5.0							
2.2 to 2.7 (5 to 6)	7.5	7.5							
Subtotal		23.25	2.75	1.25					

TABLE 10d. EXPECTED YEARLY NUMBER OF STRAIN CYCLES
(Hammer Car Impact Conditions, Head Shield At Struck End, Rear Face)

Speed Range of Coupling Impact m/s (mph)	Number of Events Per Year	Strain Cycles Per Year In Indicated Strain Ranges, μ mm/mm (μ in./in.)							
		250 to 500	500 to 750	750 to 1000	1000 to 1500	1500 to 2000	2000 to 2500	2500 to 3000	3000 to 3500
4.5 to 4.9 (10 to 11)	0.5	0.5	0.5	0.5	0.5				
4.0 to 4.5 (9 to 10)	0.75	1.5	0.5		0.5				
3.6 to 4.0 (8 to 9)	1.5	1.5	1.5	1.5					
3.1 to 3.6 (7 to 8)	3.0	6.0	3.0						
2.7 to 3.1 (6 to 7)	5.0	5.0	5.0						
2.2 to 2.7 (5 to 6)	7.5	7.5							
Subtotal		22.0	10.5	2.0	1.0				

TABLE 10e. EXPECTED YEARLY NUMBER OF STRAIN CYCLES
(Anvil Car Impact Condition, Head Shield Opposite Struck End, Front Face)

Speed Range of Coupling Impact m/s (mph)	Number of Events Per Year	Strain Cycles Per Year In Indicated Strain Ranges, μ mm/mm (μ in./in.)							
		250 to 500	500 to 750	750 to 1000	1000 to 1500	1500 to 2000	2000 to 2500	2500 to 3000	3000 to 3500
4.5 to 4.9 (10 to 11)	0.5	1.0	0.5		0.5	0.5	0.5		
4.0 to 4.5 (9 to 10)	0.75	1.5	0.75		0.75	0.75			
3.6 to 4.0 (8 to 9)	1.5	1.5	1.5	1.5	1.5				
3.1 to 3.6 (7 to 8)	3.0	3.0	3.0	3.0					
2.7 to 3.1 (6 to 7)	5.0	5.0	5.0						
2.2 to 2.7 (5 to 6)	7.5	7.5							
Subtotal		19.5	10.75	4.5	2.75	1.25	0.5		

TABLE 10f. EXPECTED YEARLY NUMBER OF STRAIN CYCLES
(Anvil Car Impact Condition, Head Shield Opposite Struck End, Rear Face)

Speed Range of Coupling Impact m/s (mph)	Number of Events Per Year	Strain Cycles Per Year In Indicated Strain Ranges, μ mm/mm (μ in./in.)							
		250 to 500	500 to 750	750 to 1000	1000 to 1500	1500 to 2000	2000 to 2500	2500 to 3000	3000 to 3500
4.5 to 4.9 (10 to 11)	0.5	0.5	0.5	0.5	0.5		0.5		0.5
4.0 to 4.5 (9 to 10)	0.75	1.5	0.75		0.75	0.75		0.75	
3.6 to 4.0 (8 to 9)	1.5	3.0	1.5		1.5	1.5			
3.1 to 3.6 (7 to 8)	3.0	3.0	3.0	3.0	3.0				
2.7 to 3.1 (6 to 7)	5.0	5.0	5.0	5.0					
2.2 to 2.7 (5 to 6)	7.5	15.0							
1.8 to 2.2 (4 to 5)	6.5	6.5							
Subtotal		34.5	10.75	8.5	5.75	2.25	0.5	0.75	0.5

TABLE 10g. EXPECTED YEARLY NUMBER OF STRAIN CYCLES
(Anvil Car Impact Condition, Head Shield At Struck End, Front Face)

Speed Range of Coupling Impact m/s (mph)	Number of Events Per Year	Strain Cycles Per Year In Indicated Strain Ranges, μ mm/mm (μ in./in.)							
		250 to 500	500 to 750	750 to 1000	1000 to 1500	1500 to 2000	2000 to 2500	2500 to 3000	3000 to 3500
4.5 to 4.9 (10 to 11)	0.5	1.0		0.5	0.5	0.5		0.5	
4.0 to 4.5 (9 to 10)	0.75	0.75	0.75	0.75	0.75		0.75		
3.6 to 4.0 (8 to 9)	1.5	3.0	1.5	1.5		1.5			
3.1 to 3.6 (7 to 8)	3.0	6.0	3.0		3.0				
2.7 to 3.1 (6 to 7)	5.0	10.0	5.0						
2.2 to 2.7 (5 to 6)	7.5	15.0							
Subtotal		35.75	10.25	2.75	4.25	2.0	0.75	0.5	

TABLE 10h. EXPECTED YEARLY NUMBER OF STRAIN CYCLES
(Anvil Car Impact Condition, Head Shield At Struck End, Rear Face)

Speed Range of Coupling Impact m/s (mph)	Number of Events Per Year	Strain Cycles Per Year In Indicated Strain Ranges, μ mm/mm (μ in./in.)							
		250 to 500	500 to 750	750 to 1000	1000 to 1500	1500 to 2000	2000 to 2500	2500 to 3000	3000 to 3500
4.5 to 4.9 (10 to 11)	0.5	0.5	0.5	0.5	0.5		0.5		
4.0 to 4.5 (9 to 10)	0.75	1.5	0.75		0.75	0.75			
3.6 to 4.0 (8 to 9)	1.5	3.0	1.5		1.5				
3.1 to 3.6 (7 to 8)	3.0	3.0	3.0	3.0					
2.7 to 3.1 (6 to 7)	5.0	5.0	5.0	5.0					
2.2 to 2.7 (5 to 6)	7.5	7.5							
Subtotal		20.5	10.75	3.5	2.75	0.75	0.5		

TABLE 11. SUMMARY OF EXPECTED YEARLY NUMBER OF STRAIN CYCLES
(Strain Ranges Adjusted for Estimate at Most Highly Stressed Location)

Condition	Strain Cycles Per Year In Indicated Strain Ranges, μ mm/mm (μ in./in.)							
	500 to 1000	1000 to 1500	1500 to 2000	2000 to 3000	3000 to 4000	4000 to 5000	5000 to 6000	6000 to 7000
<u>Front Face of Shield</u>								
Hammer Car, Shield Opposite Struck End	31.25	10.75	0.75	2.75	0.5			
Hammer Car, Shield At Struck End	23.25	2.75	1.25					
Anvil Car, Shield Opposite Struck End	19.5	10.75	4.5	2.75	1.25	0.5		
Anvil Car, Shield At Struck End	35.75	10.25	2.75	4.25	2.0	0.75	0.5	
Total	109.75	34.5	9.25	9.75	3.75	1.25	0.5	
<u>Rear Face of Shield</u>								
Hammer Car, Shield Opposite Struck End	22.0	10.75	2.0	1.25				
Hammer Car, Shield At Struck End	22.0	10.5	2.0	1.0				
Anvil Car, Shield Opposite Struck End	34.5	10.75	8.5	5.75	2.25	0.5	0.75	0.5
Anvil Car, Shield At Struck End	20.5	10.75	3.5	2.75	0.75	0.5		
Total	99.0	42.75	16.0	10.75	3.0	1.0	0.75	0.5

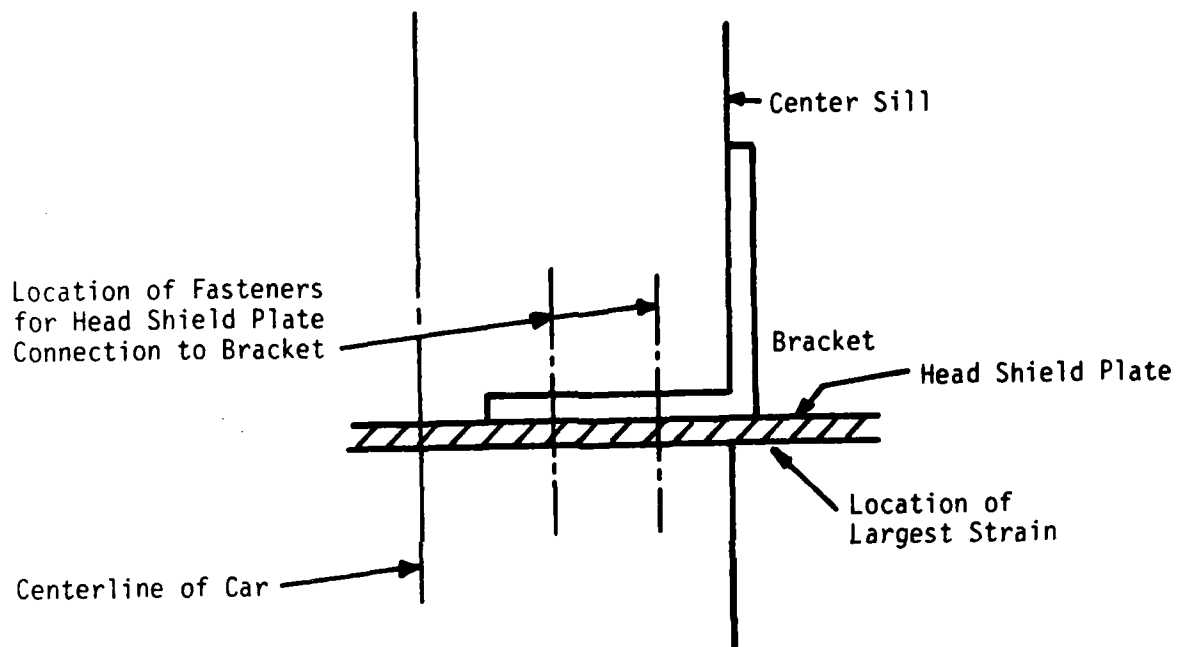


FIGURE 7. SECTION OF HEAD SHIELD PLATE AT BRACKET
SHOWING LOCATION OF LARGEST STRAIN

The AAR data establishes a fatigue limit for full strain reversals of $\pm 600 \mu \text{ mm/mm}$ at 2 million cycles. If the AAR procedures were followed to determine the fatigue damage associated with larger strain cycles, the result would be overly conservative. A general rule in fatigue design is that ± 1 percent strain ($10,000 \mu \text{ mm/mm}$) results in failure at 1000 cycles. Using the AAR procedure would result in the calculation of a stress of 338 MPa (equivalent to $1470 \mu \text{ mm/mm}$) for fatigue failure at 1000 cycles. This is a much lower strain level than would be anticipated. Therefore, another representation of the fatigue damage curve was utilized where the total strain range is related to the number of cycles to failure as follows:

$$\Delta \epsilon = \frac{A}{N^{0.12}} + \frac{B}{N^{0.6}}$$

The first term in this equation represents the elastic strain effects and the second term represents plastic strain effects. The relationship is based on the Manson-Coffin law and a form of Basquin's law (Ref 5). This equation was used to interpolate the fatigue failure curve between the two reference points: ± 1 percent strain at 1000 cycles and $600 \mu \text{ mm/mm}$ strain at 2×10^6 cycles. This curve is illustrated in Figure 8.

A linear cumulative damage law was assumed for the fatigue damage calculations. The calculation proceeded by determining the number of cycles at various levels of cyclic strain and estimating the percentage of fatigue damage for each of these levels. The damage was calculated on a yearly basis as shown in Table 12. The total expected fatigue damage was the sum of the percentages of fatigue damage in each strain range. The calculation predicted that the expected damage in a year long period is a very small percentage of the expected fatigue life, being less than 0.2 percent. From a practical standpoint it was concluded that the shield would have an infinite fatigue life.

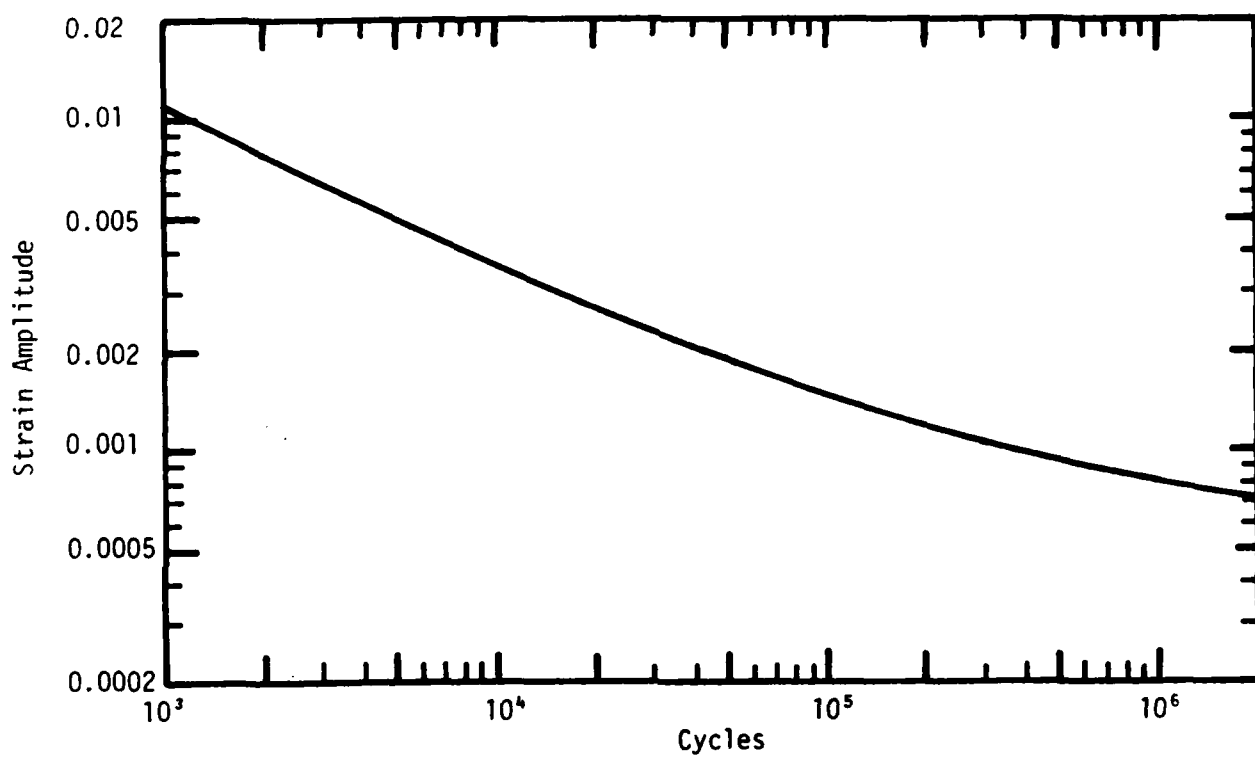


FIGURE 8. ESTIMATED FATIGUE STRENGTH CURVE FOR ASTM A242 STEEL

TABLE 12. ESTIMATED YEARLY FATIGUE DAMAGE

Range for Maximum Cyclic Strain μ mm/mm (μ in./in.)	Median of Strain Range μ mm/mm (μ in./in.)	Cycles To Failure (Fig.)	Yearly Fractional Fatigue Damage (Cycles Given in Table 11)	
			Front Face	Rear Face
500 to 1000	750	1,500,000	0.000073	0.000066
1000 to 1500	1250	170,000	0.000203	0.000257
1500 to 2000	1750	64,000	0.000145	0.000250
2000 to 3000	2500	25,000	0.000390	0.000430
3000 to 4000	3500	11,000	0.000341	0.000273
4000 to 5000	4500	6,400	0.000195	0.000156
5000 to 6000	5500	4,000	0.000125	0.000188
6000 to 7000	6500	2,900	--	0.000172
Total Estimated Yearly Fractional Fatigue Damage			0.001472	0.001786

5. CONCLUSIONS

Analysis of the test data indicated that the RAILGARD head shield provided an adequate margin of safety against the probability of accumulating significant fatigue damage over its expected life. The design appeared to be conservative from a fatigue damage standpoint and no problems were anticipated with its use.

Evaluation and analysis of the test data were restricted to the car-coupling impact environment, an environment which has previously been shown to be the most significant in the establishment of head shield fatigue damage. For a more complete appraisal of fatigue damage effects the over-the-road environment should also be considered. This environment would include the random shocks associated with train slack run-in and run-out and the vibratory responses resulting from track irregularities exciting the suspension system of the car.

The results of the work show that one cannot rely on strain gauge data alone to assess the adequacy of the head shield structure to resist fatigue damage effects. The finite element analysis used to interpolate and extrapolate the test data showed that there were large stresses at other locations on the head shield. These stresses depend on the configuration of the shield and the method of its attachment to the car. Fatigue analysis requires a means for extrapolating experimental results to other regions of the structure in order to make a thorough assessment of the probability of fatigue damage. The procedures outlined in this report showed how a dynamic finite element analysis can be used to fulfill this requirement.

ACKNOWLEDGMENT

This report received a technical review by Willis F. Jackson and William P. Wright of the Ballistic Research Laboratory. It was also approved by Edward O. Baicy, Chief of the Fragmentation Branch of the Ballistic Research Laboratory.

6. REFERENCES

1. "Specifications for Tank Cars, "Association of American Railroads, Operations and Maintenance Department, Mechanical Division
2. Jackson, W. F., " Tank Car Head Shield Evaluation, " USA Ballistic Research Laboratory Report
3. Johnson, M. R., "Fatigue Evaluation of Prototype Tank Car Head Shield," Final Report, DOT, Transportation System Center Contract TSC-1043
4. "Manual of Standards and Recommended Practices, Section C, Part II, Specifications for Design, Fabrication and Construction of Freight Cars," Association of American Railroads, Operations and Maintenance Department, Mechanical Division, 1979
5. Tetelman, A. S. and McEvily, A. J., "Fracture of Structural Materials," John Wiley and Sons, Inc., 1967

DISTRIBUTION LIST

<u>No. of Copies</u>	<u>Organization</u>	<u>No. of Copies</u>	<u>Organization</u>
12	Commander Defense Technical Info Center ATTN: DDC-DDA Cameron Station Alexandria, VA 22314	1	Commander US Army Communications Research & Development Command ATTN: DRDCO-PPA-SA Fort Monmouth, NJ 07703
1	Commander US Army Materiel Development & Readiness Command ATTN: DRCDMD-ST 5001 Eisenhower Avenue Alexandria, VA 22333	1	Commander US Army Electronics Research & Development Command Technical Support Activity ATTN: DELSD-L Fort Monmouth, NJ 07703
2	Commander US Army Armament Research & Development Command ATTN: DRDAR-TSS (2 cys) Dover, NJ 07801	2	Commander US Army Missile Command ATTN: DRSMI-R DRSMI-YDL Redstone Arsenal, AL 35809
1	Director US Army ARRADCOM Benet Weapons Laboratory ATTN: DRDAR-LCB-TL Watervliet, NY 12189	1	Commander US Army Tank Automotive Research & Development Command ATTN: DRDTA-UL Warren, MI 48090
1	Commander US Army Armament Materiel Readiness Command ATTN: DRSAR-LEP-L, Tech Lib Rock Island, IL 61299	1	Director US Army TRADOC Systems Analysis Activity ATTN: ATAA-SL, Tech Lib White Sands Missile Range, NM 88002
1	Commander US Army Aviation Research & Development Command ATTN: DRDAV-E 4300 Goodfellow Blvd. St. Louis, MO 63120	50	Department of Transportation Federal Railroad Administration Office of Rail Safety Research ATTN: Mr. D. Levine, Program Manager FRA/RRD-33 7th and D Sts., SW Washington, DC 20590
1	Director US Army Air Mobility Research & Development Laboratory Ames Research Center Moffett Field, CA 94035	5	National Railroad Passenger Corp. ATTN: E.J. Lombardi, Eng of Tests 400 N. Capitol St., N.W. Washington, DC 20001

DISTRIBUTION LIST

Aberdeen Proving Ground

Dir, USAMSAA

ATTN: DRXSY-D

DRXSY-MP, H. Cohen

Cdr, USATECOM

ATTN: DRSTE-TO-F

Dir, USACSL, Bldg. E3516, EA

ATTN: DRDAR-CLB-PA

USER EVALUATION OF REPORT

Please take a few minutes to answer the questions below; tear out this sheet, fold as indicated, staple or tape closed, and place in the mail. Your comments will provide us with information for improving future reports.

1. BRL Report Number _____

2. Does this report satisfy a need? (Comment on purpose, related project, or other area of interest for which report will be used.)

3. How, specifically, is the report being used? (Information source, design data or procedure, management procedure, source of ideas, etc.) _____

4. Has the information in this report led to any quantitative savings as far as man-hours/contract dollars saved, operating costs avoided, efficiencies achieved, etc.? If so, please elaborate.

5. General Comments (Indicate what you think should be changed to make this report and future reports of this type more responsive to your needs, more usable, improve readability, etc.) _____

6. If you would like to be contacted by the personnel who prepared this report to raise specific questions or discuss the topic, please fill in the following information.

Name: _____

Telephone Number: _____

Organization Address: _____

----- FOLD HERE -----

Director
US Army Ballistic Research Laboratory
Aberdeen Proving Ground, MD 21005

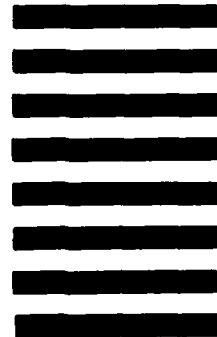


NO POSTAGE
NECESSARY
IF MAILED
IN THE
UNITED STATES

OFFICIAL BUSINESS
PENALTY FOR PRIVATE USE, \$300

BUSINESS REPLY MAIL
FIRST CLASS PERMIT NO 12062 WASHINGTON, DC
POSTAGE WILL BE PAID BY DEPARTMENT OF THE ARMY

Director
US Army Ballistic Research Laboratory
ATTN: DRDAR-TSB
Aberdeen Proving Ground, MD 21005



----- FOLD HERE -----

